national accelerator laboratory

NAL-Conf-73/59-THY

August 20, 1973

Multiperipheral and Parton Models for High Energy Processes*

HENRY D. I. ABARBANEL
National Accelerator Laboratory, Batavia, Illinois 60510

*Lectures prepared for the Canadian Institute of Particle Physics Summer School, August, 1973.

I. INTRODUCTION

In this set of lectures I wish to present a rather pedagogical view of the multiperipheral and parton models for the description of high energy collisions. My point of view will be to provide some experimental basis for each of the models; then without building elaborate versions of either model or making the student suffer the tedious details involved, I will try to extract the physics which can be discussed and often understood in the framework of the models.

Both of the models I have chosen describe extremely interesting physical phenomena at the same time as they suffer in detail from being too simple to provide a fully convincing description of the same phenomena. Since hadronic physics is almost characterized by such contradictions, one has learned to live with this unsatisfactory situation.

The first topic of discussion will be the multiperipheral model. We'll establish the basic equations of the model by studying the simplest possible version of it. Then we'll take some physical problems to apply our new knowledge to. We'll look at predictions for the n particle cross sections $\sigma_n(s)$ and after that study inclusive processes in the model.

Leaving that discussion we'll look at the parton model and investigate some of its properties as explored in deep inelastic lepton scattering. Then we'll derive some results which follow by assuming that the partons are in fact good old quarks. These results are relevant for high energy neutrino experiments at NAL.

II. MULTIPERIPHERAL MODEL

Peripheralism and Multiperipheralism

We will first turn our attention to an honorable hadronic model which attempts to put together the physics of particle production to yield results about elastic scattering, inclusive processes, and other strong interaction collision phenomenon. The model is known as the multiperipheral model and is a generalization of the very basic idea of a peripheral or exchange process familiar in two body reactions. Our development will first touch on the physics behind the detailed model of production amplitudes involved in the multiperipheral concept. Then we'll look into some of the neat properties of the multiperipheral integral equation and apply the lessons we learn to inclusive processes and other amusing physical problems. A selected (by me) set of experimental results which support the study of the multiperipheral model will be alluded to as I need them.

Let's recall the particle exchange idea which underlies almost everything we imagine to be true about collisions at high energies. Starting here and unless otherwise announced we shall deal with massive, isoscalar, scalar mesons which couple with a trilinear coupling constant g. The invariant amplitude for two-to-two scattering $p_A + p_A' \to p_B + p_B'$ (Fig. 1) depends on the two traditional invariants

$$s = (p_A + p_B)^2 \tag{1}$$

and

$$t = (p_A - p_{A'})^2. \tag{2}$$

If we evaluate the invariant amplitude T(s, t), then the elastic differential cross section is given by

$$\frac{d\sigma_{el}(s,t)}{dt} = \left| \frac{1}{8\pi\sqrt{s}} T_{el}(s,t) \right|^2, \tag{3}$$

and the total cross section is given via the optical theorem as

$$\sigma_T(s) = \frac{1}{\Delta^{1/2}(s, m_A^2, m_B^2)} \operatorname{Im}_s T_{el}(s, t=0), \tag{4}$$

where $p_A^2 = M_A^2$, $p_B^2 = M_B^2$ and

$$\Delta(x, y, z) = (x + y - z)^2 - 4xy \tag{5}$$

is the standard flux factor.

Our notation established, let us now imagine that the dynamics of T(s, t) is appropriately approximated by one scalar meson exchange of mass m (Fig. 2):

$$T(s,t) = g^2/(m^2 - t) \cdot \qquad (6)$$

This simple amplitude has really only one virtue: because of the meson propagator, $d\sigma_{el}/dt$ decreases relatively rapidly away from forward scattering, $t = 0$, and this is in fact observed experimentally. The inverse power fall off is <u>not</u> a fast enough decrease to really account for the experimental facts, but one can fudge that. Also this has a remarkably simple σ_T: $\sigma_T = 0$, since there is no imaginary part to T. These small problems aside, the fall off in t means that large t values are damped out and that in the conjugate variable to $\sqrt{-t}$, the impact parameter, large values of b are governing the structure of T_{el}. This is the peripheral idea: large space distances are involved in high energy scattering processes. The average $\sqrt{-t}$ from the peripheral amplitude (6) is $\approx m$, so $\langle b \rangle \approx 1/m$ which for the exchange of a pion would mean distances of $\approx$ 1 fermi or on the periphery of elementary particles as conventionally viewed.

Production amplitudes become important to consider when one remembers the experimental fact that $\sigma_{elastic}/\sigma_{total}$ for pp collisions, for example, is about 17 - 20 % over a wide range of collision energies from the Brookhaven and CERN AGS ($s \approx 60\,(GeV)^2$) through NAL ($s \approx 800\ (GeV)^2$) to the ISR ($s \approx 3000\ (GeV)^2$). This means that particle production plays the predominant role in high energy collisions. The multiperipheral model attempts to generalize the elementary peripheral

model to production amplitudes by ascribing simple particle exchanges (peripheral processes) to be the basic dynamical mechanism. Clearly this will be an approximation which is hard, if not impossible without a sturdy hadronic theory, to evaluate a priori. The results we'll establish will have to be defended on their own.

To see how to put these words into practice let's look at the $2 \to 3$ amplitude (Fig. 3). $T_{2\to3}(p_A + p_B \to p_1 + p_2 + p_3)$ depends on five variables which may be chosen

$$s = (p_A + p_B)^2 \tag{7}$$

$$s_1 = (p_1 + p_2)^2, \quad s_2 = (p_2 + p_3)^2, \tag{8}$$

$$\text{and} \quad t_1 = (p_A - p_1)^2, \quad t_2 = (p_B - p_3)^2. \tag{9}$$

In the peripheral spirit we imagine that for s, s_1, s_2 fixed (perhaps large) there will be considerable damping in t_1 and t_2 in the $2 \to 3$ amplitude $T(s, s_1, s_2, t_1, t_2)$ and that peripheral exchanges across these momentum transfers may yield a good approximation to the amplitude (Fig. 4). {In detail, but not in spirit, this is in contradiction to the experimental data especially in the s_i dependence. Patience will prove valuable at this point.} We then write

$$T_{2\to3} = g^3 \frac{1}{m^2 - t_1} \frac{1}{m^2 - t_2}. \tag{10}$$

No particular genius is needed to guess the $T_{2\to n}$ multiperipheral amplitudes (Fig. 5)

$$T_{2\to n}(p_A + p_B \to p_1 + \cdots p_n) = g^n \prod_{j=1}^{n} \frac{1}{m^2 - Q_j^2} \,. \tag{11}$$

The real use of this production amplitude is not in the detailed calculation of the exclusive multiple differential cross section (although it had better not be too wildly wrong about that), but instead as an approximate amplitude to put into the $2\to 2$ unitarity relation to evaluate the effect on the $2\to 2$ absorptive part from particle production. Recall that the basic peripheral absorptive part was zero. Now we generate such an absorptive part (and a non-trivial σ_T) from a model production amplitude whose major virtue, to repeat, is the built in damping in momentum transfer between produced particles. The unitarity relation in our normalization yields the two-to-two absorptive part $A(s,t) = \mathrm{Im}_s\, T(s,t)$ as a sum over products of $T_{2\to n}$

$$A(s,t) = \sum_{n=1} A_n(s,t) \tag{12}$$

where (see Fig. 6)

$$A_n(s,t) = \frac{(2\pi)^4}{2}\frac{1}{n!}\int \frac{d^4p_1}{(2\pi)^3}\,\delta(m_o^2-p_1^2)\,\theta(p_{1o})\cdots$$

$$\frac{d^4p_n}{(2\pi)^3}\,\delta(m_o^2-p_n^2)\,\theta(p_{no})\,\delta^4\Big(p_A+p_B-\sum_{j=1}^{n}p_j\Big)\times$$

$$T_{2\to n}(p_A+p_B\to p_1+\cdots+p_n)\;T^{*}_{2\to n}(p_{A'}+p_{B'}\to p_1+\cdots+p_n), \tag{13}$$

and we have taken the common mass of the produced particles to be m_o, $p_i^2 = m_o^2$.

The multiperipheral amplitudes inserted into the unitarity relation yield the multiperipheral model for A_n

$$A_n(s,t) = \frac{(2\pi)^4}{2}\int \prod_{j=1}^{n}\frac{d^4p_j}{(2\pi)^3}\,\delta(m_o^2-p_j^2)\,\theta(p_{jo})\times$$

$$\times\,\delta^4\Big(p_A+p_B-\sum_{j=1}^{n}p_j\Big)\frac{(g^2)^n}{n!}\prod_{i=1}^{n-1}\frac{1}{m^2-Q_i^2}\,\frac{1}{m^2-Q_i'^2}\Big) \tag{14}$$

where the Q_i and Q_i' are defined in Fig. 7.

Clearly the $A(s,t) = \mathrm{Im}_s T(s,t)$ will be non-zero from this procedure. This improvement on the elementary peripheral exchange will have to be fed back into the system later to generate an improved

peripheral model and, of course, an improved multiperipheral model, etc. (The faint of heart ought not embark on this easy to describe, challenging to complete iteration procedure! We'll discuss one iteration later.)

The key to success of thepresent and all multiperipheral models is that the simple structure of the assumed $T_{2\to n}$ allows one to write a recursion relation for A_n (See Fig. 8); $n \geq 2$:

$$A_n(p_A + p_B \to p_{A'} + p_{B'}) = \int \frac{d^4p}{(2\pi)^3} \delta(m_0^2 - p^2)\theta(p_0) \times$$

$$\times g^2 \frac{1}{m^2 - Q^2} \frac{1}{m^2 - Q'^2} A_{n-1}(Q + p_B \to (-Q') + p_{B'}), \tag{15}$$

where

$$p = p_A - Q = p_{B'} + Q'. \tag{16}$$

Summing on n yields under the integral.

$$A(s,t) = \sum_{n=1} A_n = \pi g^2 \delta(m_0^2 - s) +$$

$$\int \frac{d^4p}{(2\pi)^3} \delta(m_0^2 - p^2)\theta(p_0) \frac{g^2 \quad A(Q + p_B \to (-Q') + p_{B'})}{(m^2 - Q^2)(m^2 - Q'^2)}. \tag{17}$$

If we call

$$K(p_1+p_2\to p_3+p_4) = \pi g^2 \delta(m_0^2-(p_1+p_2)^2)\,\theta((p_1+p_2)_0), \tag{18}$$

we may cast the integral equation for A(s, t) into the familiar and suggestive form

$$A(p_A+p_B\to p_{A'}+p_{B'}) = K(p_A+p_B\to p_{A'}+p_{B'}) + \frac{2}{(2\pi)^4}\int d^4p\, K(p_A+(-Q)\to p_{A'}+Q')\, G_0(Q,Q')\times A(Q+p_B\to(-Q')+p_{B'}), \tag{18}$$

where $G_0(Q, Q')$ is the free propagator

$$G_0(Q,Q') = [(m^2-Q^2)(m^2-Q'^2)]^{-1}. \tag{19}$$

This is reminiscent of the Bethe-Salpeter equation derived in quantum field theory where K would be taken to be the two particle irreducible part.

Generalizations of the very elementary multiperipheral model given here consist in essence of changes in K and G_0. For example, K might be generalized to a distribution over the invariant energy carried through it and the masses of the legs

$$K(p_1+p_2\to p_3+p_4) = K((p_1+p_2)^2, (p_1-p_3)^2, p_i^2), \tag{20}$$

and G_o might be generalized to refer to propagation of spinning particles or perhaps Reggeons.

Diagonalizing the Multiperipheral Integral Equation

As it stands the equation for A(s,t) is easy in principle to solve because the phase space restrictions in the integrals truncate the iterative Neumann or Born series after a finite number of steps. We will be interested in the behavior of A(s,t) for large s and fixed t, however, and it proves very convenient to turn the truncating equation for A(s,t) into a serious integral equation for an integral transform of A which eliminates s in favor of its conjugate: the complex angular momentum. This turns (18) into a two dimensional equation for $t \neq 0$ and a one dimensional equation at $t = 0$.

We will consider the case $t = 0$. This has clear relevance for $\sigma_T(s)$ and will be used in all our applications. Define variables by those appearing in Fig. 9. Then after some Jacobian activity one may write (18) as an equation over invariants

$$A(s,u,v) = K(s,u,v) + \frac{2}{(2\pi)^4} \int_{L^2}^{(\sqrt{s}-L)^2} ds' \int_{L^2}^{(\sqrt{s'}-L)^2} ds_0 \int_{U_-}^{U_+} du' \times$$

$$\times \frac{K(s_0,u,u')\,A(s',u',v)}{(m^2-u')^2} \frac{1}{J} \,, \qquad (21)$$

where

$$\frac{1}{\mathcal{J}} = \int d^4 q \; \delta(q^2 - u') \, \delta((q + p_B)^2 - s') \, \delta((p_A - q)^2 - s_0), \tag{22}$$

and L is just some lower bound on any invariant energy. $U_\pm$ are complicated functions determined by the various phase space restrictions; for the record we record them here

$$U_\pm = u + m_0^2 - \frac{(s+u-v)(s+m_0^2-s')}{2s} \pm$$

$$\Delta^{1/2}(s,u,v)\,\Delta^{1/2}(s,m_0^2,s')\,/2s \,. \tag{23}$$

Having changed variables we now may eliminate all the s variables by defining the integral (Laplace)transforms

$$A(l,u,v) = \int_{L^2}^{\infty} ds \; e^{-(l+1)\vartheta(s,u,v)} \; A(s,u,v), \tag{24}$$

and

$$K(l,u,v) = \int_{L^2}^{\infty} ds \; e^{-(l+1)\vartheta(s,u,v)} \; K(s,u,v), \tag{25}$$

where

$$\cosh\vartheta(s,u,v) = \frac{s-u-v}{2\sqrt{uv}}. \tag{26}$$

It is convenient here to artifically take u and v to be negative and later, after solving for $A(\ell, u, v)$, continuing by hand back to time like external momenta.

Transforming (21) with elaborate care given to all limits of integration, we arrive at the bona fide one dimensional integral equation

$$A(\ell,u,v) = K(\ell,u,v) + \frac{1}{16\pi^3(\ell+1)} \int_{-\infty}^{0} \frac{du'}{(m^2-u')^2} K(\ell,u,u')\, A(\ell,u',v). \tag{27}$$

For the particular inhomogeneous term we have been discussing above where

$$K(s,u,v) = \pi g^2 \delta(m_0^2 - s), \tag{28}$$

we have

$$K(\ell,u,v) = \pi g^2 e^{-(\ell+1)\vartheta(m_0^2,u,v)}, \tag{29}$$

$$= \left[\frac{m_0^2 - u - v + \Delta^{1/2}(m_0^2,u,v)}{2\sqrt{uv}}\right]^{-\ell-1}. \tag{30}$$

Before examining the solution to Eq. (27) in some special cases, let's review what we've done with our unbelievably clever integral

transform and see what we can expect from the solution to such an equation. The diagonalization procedure which eliminated the s variables leaving us an integral equation in momentum transfers or masses alone (the u or Q^2 variables) is just a fancy trick for taking the ordinary partial wave amplitude in the channel where t (here zero) is the invariant energy and continuing the answer in the angular momentum ℓ. In general taking a partial wave projection reduces a four dimensional integral equation (Eq. 18) to a two dimensional integral equation as one integrates out the polar and azimuthal angle dependence on the t-channel. In the special case of t = 0 the partial wave corresponds to an 0(4) projection rather than an 0(3) projection and one has two polar angles and one azimuthal angle to integrate out; this takes a four dimensional equation, then we recover the full absorptive amplitude by Laplace inversion

$$A(s,u,v) = \int_{c-i\infty}^{c+i\infty} \frac{d\ell}{2\pi i} \frac{e^{(\ell+1)\vartheta(s,u,v)}}{2\sqrt{uv}\sinh\vartheta(s,u,v)} A(\ell,u,v), \qquad (31)$$

where, as usual, Re c is to the right of any singularities in ℓ.

What might we expect for the analytic structure in ℓ of an A(ℓ, u, v) which satisfies Eq. (27)? Write it as a matrix equation in u, u′, v space

$$A(\ell) = K(\ell) + \lambda(\ell) K(\ell) G_0 A(\ell), \qquad (32)$$

whose formal solution is

$$A(\ell) = \left[1 - \lambda(\ell) K(\ell) G_0\right]^{-1} K(\ell). \tag{33}$$

If (formally) $(1 - \lambda K G_0)^{-1}$ develops a zero in ℓ, then $A(\ell)$ develops a pole in ℓ. A pole in $A(\ell)$ of the form

$$A(\ell) = \tilde{\gamma} / (\ell - \alpha_0), \tag{34}$$

leads to a behavior of $A(s,u,v)$ of the form

$$A(s,u,v) \underset{s\to\infty}{\sim} \gamma s^{\alpha_0}, \tag{35}$$

closing the ℓ contour to the left about the pole at $\ell = \alpha_0$. More complicated structures for $A(\ell)$ give rise to extra log s factors in A(s). This is our first important result from the multiperipheral model. The elementary approximation to the production amplitude $T_{2\to n}$ which leads to thekey recursion relation (15) can lead to <u>power behavior in $A(s, t = 0)$</u> which is quite different from the input behavior of the basic peripheral amplitude. The total cross section is

$$\sigma_T(s) \sim \gamma s^{\alpha_0 - 1}. \tag{36}$$

{ The value of α_0 is determined as a function of g^2 (or K in general) and can easily be non-integral. } This is the phenomenon of <u>Regge behavior</u> for $2 \to 2$ amplitudes which is a quite desirable property. Solving for

α_o is quite difficult in general (yea, probably impossible).

Before we pass on to instructive special cases, let's look again at the formal structure of (32). Suppose the "matrix" $\lambda(\ell)\, K(\ell)\, G_o$ has a complete set of eigenvectors $\psi_n(\ell, u)$ and associated eigenvalues $\sigma_n(\ell)$

$$\lambda(\ell) \int_{-\infty}^{0} du'\, K(\ell, u, u')\, G_o(u')\, \psi_n(\ell, u') = \sigma_n(\ell)\, \psi_n(\ell, u), \tag{37}$$

and imagine the σ_n are non-degenerate.

Writing (as we may under certain conditions which I let the reader look up in his favorite books) $A(\ell, u, v)$ in the form

$$A(\ell, u, v) = \sum_n a_n(\ell)\, \psi_n(\ell, u)\, \psi_n^*(\ell, v), \tag{38}$$

and similarly for $K(\ell, u, v)$

$$K(\ell, u, v) = \sum_n k_n(\ell)\, \psi_n(\ell, u)\, \psi_n^*(\ell, v), \tag{39}$$

then

$$a_n(\ell) = \frac{k_n(\ell)}{1 - \sigma_n(\ell)} \tag{40}$$

Suppose now the largest of the $\sigma_n(\ell)$, call it $\sigma_1(\ell)$, passes through one

for some value $\ell = \alpha_o$. In the neighborhood of $\ell = \alpha_o$

$$\sigma_1(\ell) = 1 + (\ell - \alpha_o) \left.\frac{\partial \sigma_1(\ell)}{\partial \ell}\right|_{\ell=\alpha_o} + \cdots \tag{41}$$

and

$$a_1(\ell) = \frac{k_1(\alpha_o)}{-\sigma_1'(\alpha_o)(\ell - \alpha_o)} \tag{42}$$

and

$$A(\ell, u, v) = \frac{\gamma_1(\alpha_o)\,\psi_1(\alpha_o, u)\,\psi_1^*(\alpha_o, v)}{\ell - \alpha_o} . \tag{43}$$

We have assumed $k_1(\alpha_o)$ is non-singular to α_o, which happens to be true for our model $K(\ell, u, v)$ Eq. (30).

We have arrived at an additional very important piece of information. At a pole of $A(\ell, u, v)$ arising from the multiperipheral integral equation, the residue of the pole factorizes. Here into a product of a function of u and a function of v. This is actually quite a general property of Regge poles which follows from extended unitarity in the channel where the Regge pole is exchanged. So the apparatus we have set up yields (at t = 0) factorizable poles in complex angular momentum. That is a general feature of whole classes of multiperipheral models and is, in a certain sense, the whole general context of the models.

To see more of the detail which may be of interest let's look at the special case $m_o = 0$ of our elementary multiperipheral model.

The kernel function K(ℓ, u, v) becomes

$$K(\ell, u, v) = \pi g^2 \left[\sqrt{\frac{-u}{-v}}\right]^{\ell+1}, \quad u > v, \tag{44}$$

$$= \pi g^2 \left[\sqrt{\frac{-v}{-u}}\right]^{\ell+1}, \quad v > u. \tag{45}$$

This simple kernel allows one to turn the integral equation for A into a differential equation which happens to be a hypergeometric equation. The important fact about the solution is the position of the leading pole in ℓ at

$$\alpha_0(g^2) = -\frac{3}{2} + \sqrt{\frac{1}{4} + g^2/16\pi^2 m^2}\ . \tag{46}$$

Indeed there are only poles in ℓ trailing this leading pole by integer steps.

Another case where one may solve the multiperipheral integral equation is for large m_o in which situation the inhomogeneous term K becomes to a good approximation separable. Indeed one finds that there are both a separable upper bound and a separable lower bound approximation to K

$$K_L(\ell, u, v) \leq K(\ell, u, v) \leq K_U(\ell, u, v), \tag{47}$$

with

$$K_L(\ell,u,v) = \pi g^2 \left[\frac{\sqrt{uv}}{m_0^2}\right]^{\ell+1} \left\{\frac{m_0^4}{(m_0^2-u)(m_0^2-v)}\right\}^{\ell+1}, \quad (48)$$

and

$$K_U(\ell,u,v) = \pi g^2 \left\{\frac{uv}{m_0^4} \quad \frac{m_0^2}{m_0^2-2u} \quad \frac{m_0^2}{m_0^2-2v}\right\}^{\frac{\ell+1}{2}}. \quad (49)$$

The multiperipheral equation with a separable kernel is very easy to solve. Suppose we have

$$K(\ell,u,v) = f_\ell(u)\, f_\ell(v) \quad (50)$$

as in the K_u or K_L examples. Then

$$A(\ell,u,v) = f_\ell(u) f_\ell(v) + \frac{1}{16\pi^3(\ell+1)} \int_{-\infty}^{0} \frac{du'}{(m^2-u')^2} f_\ell(u) f_\ell(u') A(\ell,u',v), \quad (51)$$

and

$$A(\ell,u,v) = f_\ell(u) f_\ell(v) \Big/ \left[1 - \frac{1}{16\pi^3(\ell+1)} \int_{-\infty}^{0} \frac{du'\, f_\ell(u')^2}{(m^2-u')^2}\right]. \quad (52)$$

The vanishing of the denominator gives rise to poles or more complicated structures in ℓ. In the upper and lower bound examples we just gave, one finds that the zeroes of the denominator are given for K_L by

$$1 = \frac{g^2}{16\pi^2 m_o^2 (\lambda+1)} \eta \left(\frac{2}{2+\eta}\right)^2 \frac{\Gamma^2(\lambda+2)}{\Gamma(2\lambda+4)} {}_2F_1\left(\tfrac{1}{2}, \tfrac{3}{2}; \lambda+\tfrac{5}{2}; \left(\frac{1+\eta}{1-\eta}\right)^2\right), \quad (53)$$

and for K_u

$$(\ell+1)(\ell+2) = \frac{g^2}{8\pi^2 m_o^2} {}_2F_1(2,1;\lambda+3;1-2\eta). \quad (54)$$

where $\eta = M^2/M_o^2$. η should be a small quantity for the K_L or K_u approximations to be valid. If $M = M_\pi$ (pion exchange along the multiperipheral chain) and $M_o = M_\rho$ (ρ production), then $\eta \approx 1/5$ and one may solve (53) or (54) by expanding in η.

The point of presenting these, often complicated, examples is to indicate that in general the position of the output pole is not a polynomial in g^2 but more involved. This has some physical consequences as we'll soon see. In each example the leading pole as a function of g^2 retreats to $\ell = 1$ at $g^2 = 0$

$$\alpha_o(g^2) = -1 + O(g^2/m^2). \quad (55)$$

The Regge pole output of these simplest multiperipheral equations predicts strict power behavior in s for two-to-two absorptive parts or total cross sections. In fact experimental evidence gathered at the CERN-ISR indicates that there are definite log s terms in σ_T. The

precise nature of these log pieces is at this writing still a matter of debate but their presence at all implies that the singularity structure in ℓ must be more elaborate than sets of simple poles. With this in mind we must eventually modify the elementary equations we have derived. If $\sigma_T(s)$ is rising in s in a log s or $(\log s)^2$ fashion, then the ℓ -plane structure will be a double pole or triple pole at $\ell = +1$. If the behavior is to approach a constant σ_T asymptotically

$$\sigma_T(s) \sim a + b/\log s + c/(\log s)^2 + \cdots \quad (56)$$

then there will be a pole with $\alpha_o = 1$ and cuts in ℓ whose branch point at $t = 0$ is at $\ell = 1$. In each case the point $\ell = +1$ is singled out for attention. To reach $\ell = +1$ from $\ell = -1$ where our multiperipheral models begin for small g^2 means that the physics of high energy scattering demands a strong coupling solution-like our exact solutions-to those equations.

Applications of the t = 0 Multiperipheral Model

An interesting physical question one may address in the framework of our model is that of the behavior of the n-prong cross section $\sigma_n(s)$

$$\sigma_n(s) = \frac{1}{\Delta^{1/2}(s, m_A^2, m_B^2)} A_n(s, t=0), \tag{57}$$

$$\sigma_T(s) = \sum_n \sigma_n(s). \tag{58}$$

For example, consider the first moment of the probability distribution $\sigma_n(s)/\sigma_T(s)$

$$\langle n \rangle = \sum_n n \sigma_n(s) \Big/ \sigma_T(s) \tag{59}$$

which one recognizes as the mean multiplicity of produced particles. Note

$$\sigma_T(s)\langle n \rangle = \sum_{n=1} n \sigma_n(s) = \frac{1}{\Delta^{1/2}(s, m_A^2, m_B^2)} \sum_{n=1} n A_n(s, 0). \tag{60}$$

Now

$$A_n(l, u, v) = \frac{1}{16\pi^3(l+1)} \int_{-\infty}^{0} \frac{du'}{(m^2 - u')^2} K(l, u, u') A_{n-1}(l, u', v), \quad n \geq 2, \tag{61}$$

where

$$A_1(l, u, v) = \int_{L^2}^{\infty} ds\, e^{-(l+1)\delta(s,u,v)} A_n(s, u, v), \tag{62}$$

and the basic recursion relation (15) has been employed. It follows

that

$$A_n(l,u,v) = \frac{1}{16\pi^3(l+1)} \int_{-\infty}^{0} \frac{du'}{(m^2-u')^2} A_k(l,u,u') A_{n-k}(l,u',v),$$

$$\text{for } k = 1, 2, \cdots, n-1, \tag{63}$$

so

$$\sum_{n=1}^{\infty} n A_n(l,u,v) = \sum_{n=1}^{\infty} \left\{ \sum_{k=1}^{n-1} \frac{1}{16\pi^3(l+1)} \int_{-\infty}^{0} \frac{du'}{(m^2-u')^2} A_k(l,u,u') A_{n-k}(l,u',v) \right. \tag{64}$$

$$\left. + A_n(l,u,v) \right\}$$

$$= \frac{1}{16\pi^3(l+1)} \int_{-\infty}^{0} \frac{du'}{(m^2-u')^2} A(l,u,u') A(l,u',v) + A(l,u,v). \tag{65}$$

We have then

$$\langle n \rangle = \int_{c-i\infty}^{c+i\infty} \frac{dl}{2\pi i} \frac{e^{(l+1)\delta(s,u,v)}}{2\sqrt{uv}\,\sinh\delta} \sum_{n=1}^{\infty} n A_n(l,u,v) \Big/ A(s,t=0). \tag{66}$$

Suppose there is a pole in $A(\ell, u, v)$ at $\ell = \alpha_0$:

$$A(l,u,v) = f(u) f(v) / l - \alpha_0. \tag{67}$$

$A(s, t = 0)$ behaves for large s as

$$A(s, t=0) \underset{s\to\infty}{\sim} \frac{f(u)}{\sqrt{-u}} \frac{f(v)}{\sqrt{-v}} e^{\alpha_0 \delta(s,u,v)} \tag{68}$$

$$= \frac{f(u) f(v)\, s^{\alpha_0}}{(\sqrt{uv})^{\alpha_0+1}} . \tag{69}$$

While the numerator of (62) behaves as

$$\frac{f(u) f(v)\, s^{\alpha_0}}{(\sqrt{uv})^{\alpha_0+1}} \left[\log \frac{s}{\sqrt{uv}} \int_{-\infty}^{0} \frac{du'}{16\pi^3(\alpha_0+1)} \frac{f(u')^2}{(m^2-u')^2} + 1 \right]. \tag{70}$$

The behavior of $\langle n \rangle$ is thus predicted to be

$$\langle n \rangle \sim A \log s + B. \tag{71}$$

a result which depends crucially on there being a simple pole in ℓ and on the recursion relation (15) Precisely the same reasoning leads one to discover that

$$\langle n(n-1) \rangle \sim (A \log s + C)^2 , \tag{72}$$

and so forth for the higher combinatorial moments

$$\langle n(n-1)\cdots(n-k+1) \rangle = (A \log s + D_k)^k . \tag{73}$$

This is an interesting result because it shows that the distribution

$\sigma_n(s)$ at fixed s will look like a Poisson distribution as $s \to \infty$, but only in a logarithmic fashion. To see this recall the form of a Poisson distribution

$$P_n = \frac{e^{-\langle n \rangle} \langle n \rangle^n}{n!} . \tag{74}$$

Form the generating function

$$G(z) = \sum_{n=0}^{\infty} z^n P_n = e^{(z-1)\langle n \rangle} \tag{75}$$

and note that $\langle n(n-1)\ldots(n-k+1) \rangle$ for this distribution is given by

$$\langle n(n-1)\cdots(n-k+1) \rangle = \frac{\partial^k}{\partial z^k} G(z) \Big|_{z=1} = (\langle n \rangle)^k . \tag{76}$$

This is true as $\log s \to \infty$ for the multiperipheral σ_n, but <u>only</u> then.

Pursuing this slightly further, note that

$$A(s, t=0) = \sum_n (g^2)^n a_n(s, t=0) \tag{77}$$

for the multiperipheral models we have been discussing. Now

$$\langle n \rangle = g^2 \left[\frac{\partial}{\partial g^2} A(s, t=0) \right] / A(s, t=0) , \tag{78}$$

and similarly for higher moments. But for large s

$$A(s, t=0) \sim \gamma\, e^{\alpha_0(g^2) \log s} . \tag{79}$$

From our arithemetic on the Poisson distribution we see that only in the case that $\alpha_o(g^2)$ is linear in g^2 will we find a strict Poisson distribution. This is clearly not the case in the soluble examples we discussed before since $\alpha_o(g^2)$ has actually a complicated dependence on g^2. So even though asymptotically we may look for a Poisson distribution, at any finite energies the multiperipheral model leads one to expect sizeable deviations from the simple result.

The physics of this is easy to understand. When $\alpha_o(g^2)$ is taken to be linear in g^2, we are working in the weak coupling limit. In this $g^2 \to 0$ limit the production of any given particle becomes quite independent of the production of any other particle. This is precisely the circumstance under which one expects a Poisson distribution. Similarly as $\log s \to \infty$, the factorizablilty of the exchanges in the multiperipheral chain along with the ability to neglect masses and recoils from the production of an additional particle again lead to the statistical independence needed for a Poisson distribution.

Another very interesting set of physical phenomena can be discussed with our knowledge of the t=0 multiperipheral equation. Consider those processes in which one detects exactly one of themany (identical, spinless, etc) particles produced in our usual A+B collision and sums over the phase space of the rest. (Fig. 10) This defines the single particle inclusive cross section

$$E_1 \frac{d\sigma(A+B\to 1+X)}{d^3p_1} = \sum_{n=2}^{\infty} \int \frac{d^3p_2}{E_2} \cdots \frac{d^3p_n}{E_n} \frac{1}{(n-1)!} \times$$

$$\times \delta^4\left(p_A + p_B - p_1 - \sum_{j=2}^{n} p_j\right) \frac{d\sigma(A+B\to 1+2+\cdots+n)}{d^3p_2/E_2 \cdots d^3p_n/E_n} . \tag{80}$$

From the multiperipheral point of view the produced particle can have come from one of two--more or less distinct--places in the production chain: (a) the ends or near the ends or (b) the middle or central region.

Let's look at the ends first. Squaring the amplitude in Fig. 10 we find that if the particle came off the end of the chain as in Fig. 11, then the inclusive cross section is given by

$$E_1 \frac{d\sigma}{d^3p_1} = \frac{g^2}{16\pi^3} \frac{1}{(m^2-Q^2)^2} \frac{A(Q+p_A\to(-Q)+p_A)}{\Delta^{1/2}(s, m_A^2, m_B^2)} , \tag{81}$$

where A is the multiperipheral absorptive amplitude.

The inclusive cross section depends on three variables. It is convenient to choose them as follows: define the longitudinal rapidity of any particle by

$$y_i = \frac{1}{2} \log\left[\frac{E_i + p_{\ell i}}{E_i - p_{\ell i}}\right] , \tag{82}$$

where $p_{\ell i}$ is the particle momentum along the beam direction (longitudinal momentum) and E_i is the energy. The rapidity is the longitudinal boost angle taking the particle from rest to energy E_i. Now label every particle by its y_i and its transverse momentum p_{Ti}. Phase space is simply

$$\frac{d^3p_i}{E_i} = dy_i\, d^2p_{Ti} \tag{83}$$

The three variables we'll use for the inclusive cross section will be the over all rapidity in the center of mass system defined by

$$p_A = m(\cosh Y, 0, 0, \sinh Y) \tag{84}$$

and

$$p_B = m(\cosh Y, 0, 0, -\sinh Y), \tag{85}$$

setting $m_A = m_B = m$. The energy s is

$$s = (p_A + p_B)^2 = 2m^2(1 + \cosh 2Y) \tag{86}$$

or

$$s \approx m^2 e^{2Y}. \tag{87}$$

for large s or Y. We parameterize p_1 by

$$p_1 = (m_{T1}\cosh y_1, p_{T1}, 0, m_{T1}\sinh y_1), \tag{88}$$

where

$$m_{T1} = \sqrt{m^2 + p_{T1}^2} \tag{89}$$

The momentum transfer Q^2 in (81) is given by

$$Q^2 = 2m^2 - 2m m_{T1} \cosh(Y - y_1) \tag{90}$$

and as s (or Y) goes to infinity, it will remain finite if p_{T1} and the rapidity difference $Y-y_1$ are held fixed. We, of course, want Q^2 to remain finite so that the multiperipheral assumptions apply.

When p_{T1} and $Y-y_1$ are fixed, the invariant energy in the absorptive part in (81)

$$(Q+p_B)^2 = m^2 + Q^2 + m^2 \cosh 2Y - m m_{T1} \cosh(2Y + (y_1 - Y)) \tag{91}$$

also grows. We know from our previous work that $A(Q+p_B \to (-Q)+p_B)$ then behaves as

$$A(Q+p_B \to (-Q)+p_B) \sim [(p_B+Q)^2]^{\alpha_0} f_A(Q^2) f_B(p_B^2) \tag{92}$$

$$\sim e^{2Y\alpha_0} g_A(p_{T1}, Y-y_1) f_B(p_B^2) \tag{93}$$

In the limit then as Y (or s) becomes large, while p_{T1} and $Y-y_1$ are fixed

$$\frac{d\sigma}{dy_1 d^2p_{T1}} \sim (e^{2Y})^{\alpha_0 - 1} \; h_A(p_{T1}, Y-y_1) \, f_B(p_B^2). \tag{94}$$

If we divide by $\sigma_T^{AB}(Y)$ which behaves as

$$\sigma_T^{AB}(Y) \sim (e^{2Y})^{\alpha_0 - 1} \, f_A(p_A^2) \, f_B(p_B^2), \tag{95}$$

then we expect

$$\frac{1}{\sigma_T^{AB}(Y)} \frac{d\sigma(A+B \to 1+X)}{dy_1 d^2p_{T1}} \underset{\substack{Y-y_1, p_{T1} \\ \text{fixed}}}{\sim} \frac{h_A(p_{T1}, Y-y_1)}{f_A(p_A^2)} . \tag{96}$$

as shown in Fig. 11.

This result predicts that if we measure the momentum of the detected particle #1 and let the incident energy in the collision increase holding p_{T1} and $Y-y_1$ fixed, then the ratio $\sigma_T^{-1} \, d\sigma/dy_1 \, d^2p_{T1}$ approaches a finite limit, regardless of the value of α_o. There are two important features here which are general features of Regge pole exchange and do not rely in detail on the multiperipheral model: (a) The same value of the Regge intercept α_o appears in σ_T and $d\sigma/dy_1 d^2 p_{T1}$ because the physics of multiparticle states which builds up (invariant energy)$^{\alpha_o}$ behavior is the same whether or not we remove and detect one (or a finite number) selected particle. (b) Because the residue of the pole factorizes, the ratio in Eq. (96) is <u>independent of particle B</u>.

The range of rapidity y_1 which is available by energy momentum conservation is essentially

$$-Y \leq y_1 \leq Y \tag{97}$$

When $y_1 \approx Y$, the detected particle is more or less moving in the direction of particle A and is called a fragment of A. When $y_1 \approx -Y$, it is called a fragment of B. It should be clear that if we select particle 1 to have $y_1 + Y$ fixed, p_{T1} fixed as $Y \to \infty$, then a limit like (96) will hold with the names A and B switched. The limit (96) is known as the A fragmentation limit; the other "end of the chain" limit is the B fragmentation limit. Each of these limits has been observed to occur in a large variety of particle collisions over energy ranges from $s \approx 60(\text{GeV})^2$ through NAL to the ISR at $s \approx 3000\,(\text{GeV})^2$; that is all ratios like (96) have been observed to become effectively independent of s.

Our second kind of limit involves the detected particle coming from the center of the multiperipheral chain as in Fig. 12. The cross section for this is given by

$$\Delta^{1/2}(s, m_A^2, m_B^2)\frac{d\sigma}{dy_1 d^2p_{T1}} = \int \frac{d^4Q_1\, d^4Q_2}{(m^2-Q_1^2)^2(m^2-Q_2^2)^2} A(p_A + (-Q_1) \Rightarrow p_A + Q_1) \times$$

$$\times \frac{g^2}{16\pi^3}\delta^4(p_1 + Q_2 - Q_1)\, A(p_B + Q_2 \Rightarrow p_B + (-Q_2)). \tag{98}$$

To keep particle 1 in the central region where (98) applies we must hold p_{T1} and y_1 fixed as $Y \to \infty$; that is, in rapidity space it must stay away from the ends. Holding p_{T1} fixed keeps the momentum transfers Q_1^2 or Q_2^2 from growing and damping out the contribution we have selected. As $Y \to \infty$ with y_1 and p_{T1} fixed the energies in each of the absorptive parts in (98) grows and the inclusive cross section becomes (see Fig. 13)

$$\frac{d\sigma}{dy_1 d^2p_{T1}} \underset{\substack{y_1, p_{T1} \text{ fixed}}}{\sim} \frac{e^{\alpha_0(Y-y_1)} e^{\alpha_0(Y+y_1)}}{e^{2Y}} \beta_A(p_A^2) g(p_{T1}) \beta_B(p_B^2) \quad (99)$$

where $g(p_{T1})$ is some elaborate function depending on the details of the multiperipheral model but, because of factorization, not on particles A or B. Dividing by $\sigma_T^{AB}(Y)$, Eq. (95), again we see

$$\frac{1}{\sigma_T^{AB}(Y)} \frac{d\sigma}{dy_1 d^2p_{T1}} \underset{\substack{y_1, p_{T1} \text{ fixed}}}{\sim} g(p_{T1}) \quad (100)$$

that is, it is <u>independent of A and B of α_o and of y_1</u>: a very strong result indeed.

If we now plot the distribution $\sigma_T^{-1}\, d\sigma/dy_1\, d^2p_{T1}$ in y_1 space we expect, for $Y \to \infty$ something like the shape in Fig. 14; namely, a y_1 dependence near the ends of phase space (or the multiperipheral chain) and y_1 independence in the middle. Indeed in pp collisions at the

CERN-ISR one sees essentially this shape with the central plateau becoming flatter and flatter as Y(or s) increases. Thus the elementary predictions of the multiperipheral idea seem experimentally verified.

Let us draw one further consequence of our view of the inclusive process. By the definition in Eq. (80), if one integrates $d\sigma/dy_1 d^2p_{T1}$ over all of phase space, he finds

$$\int dy_1 d^2p_{T1} \frac{d\sigma^{AB}}{dy_1 d^2p_{T1}} = \langle n_1 \rangle \sigma_T^{AB}(s), \tag{101}$$

where $\langle n_1 \rangle$ is the multiplicity as a function of Y of particles of type 1 produced in AB collisions. The appearance of $\langle n_1 \rangle$ is easy to understand since each time particle 1 occurs in the final state of an AB collision, it is counted as a contribution to the inclusive cross section. If a particle of type #1 appears two, three,... times, that event is counted two, three,... times.

If we do the integration in (101) using our results for $\frac{1}{\sigma_T} d\sigma/dy_1 d^2 p_{T1}$ remembering that the distributions in p_{T1} are damped strongly, then we find

$$\langle n_1 \rangle = A'Y + B' = A \log s + B \tag{102}$$

as before. The coefficient of the log s is now directly related to the height of the rapidity plateau.

We will terminate our discussion of the multiperipheral model

with the mention of a number of interesting detailed topics which time does not allow us to cover. First, one can explore the very ends of the phase space in rapidity where the energy between particle 1 and any particle in the anything is so large that a Regge pole exchange rather than a simple particle propagator is expected. Then one will be looking at the generalization of Fig. 11 seen in Fig. 15 where the triple Reggeon formula is significant. Second, one may ask how the structure of the partial wave amplitude $A(\ell, u, v)$ (for $t = 0$) is altered when Regge poles are exchanged along the sides of the multiperipheral chain. This leads to branch points in the ℓ-plane. Making the model consistent in the sense of ℓ-plane input equals ℓ-plane output then becomes a non-trivial and thus far unsolved problem. We will hear more about this from Professor Zachariasen at this summer school. Third, one may investigate within the framework we have established the rate at which the inclusive limits in (96) and (100) are approached. This rate is governed by both the detailed dynamics of the model and the next leading trajectory intercept below α_o. Fourth, one may address the significant problem of the magnitude of α_o. We have seen that in our simplest models α_o begins as a function of g^2 at $\ell = -1$, yet in the world of physics one needs $\alpha_o \cong 1$. Changing the basic particles building the multiperipheral chain into spinning objects or Reggeons allows one to get closer to $\alpha_o = 1$ to start with. Getting all the way has never been achieved. Finally, one may look at the structure of two or more particle inclusive processes to study

correlations among produced particles and to learn a more physically realistic version of the $T_{2\to n}$ production amplitude which is used in the unitarity relation to generate the model itself.

It is possible at this time to end on a rather optimistic note about the multiperipheral model. The very high energy data from NAL and the CERN-ISR have remarkably served to confirm in detail the predictions of the model-even beyond the realistic expectations of multiperipheral enthusiasts. Accepting the general mode of thought here as correct then, one is strongly encouraged to refine and push the whole structure.

III. PARTON MODELS

The parton model is founded on the idea that a hadron is made up of point like constituents (partons) which, perhaps, are the quanta of a field theory underlying strong interactions. Of course, these quanta are not always individually observable since they interact strongly with each other, so that a description of hadrons in terms of them becomes significant when one can envision a physical situation which somehow emphasizes their point like nature. The natural and cleanest such situation occurs when one hits the hadron with a point like probe such as a photon or weak current "beam" and makes this probe on a time scale which is short relative to the interaction times of the partons themselves.

This is the case in deep inelastic lepton scattering as studied in the electron experiments at SLAC and the muon and neutrino experiments at NAL. We will begin our discussion of partons by recalling the salient features of those experiments.

Inelastic lepton scattering is an inclusive experiment of the form lepton + proton → lepton + anything. In the approximation that the reaction takes place via one photon or one weak current exchange we have the kinematic stiuation seen in Fig. 16. The amplitude for this process is proportional to

$$j_\alpha^l \, D^{\alpha\beta}(q^2) \langle X | J_\beta^h(0) | p \rangle \tag{103}$$

where j_α^l is the leptonic current

$$j_\alpha^l = \bar{u}_{l'} \gamma_\alpha u_l \tag{104}$$

for electromagnetism, and

$$j_\alpha^l = \bar{u}_{l'} \gamma_\alpha (1-\gamma_5) u_l \tag{105}$$

for weak transitions. The vector meson propagator $D^{\alpha\beta}(q^2)$ connects the lepton current to the hadronic matrix element of the hadron current operator $J_\beta^h(0)$. The guts of the process are in this matrix element since, up to higher order weak or electromagnetic corrections, we presume j_α^l to be known.

Concentrate now on the electromagnetic case and work in the laboratory system of the target proton of momentum p

$$p = (m, 0, 0, 0), \tag{106}$$

and let the initial and final energy of the leptons be E and E' respectively. The momentum transfered to the hadrons is

$$q^2 = -4EE' \sin^2 \vartheta/2, \tag{107}$$

where ϑ is the angle through which the lepton is scattered. In this notation the cross section becomes

$$\frac{d\sigma(l+p \to l' + \text{anything})}{-dE'\, dq^2} = \frac{4\pi\alpha^2}{(q^2)^2} \frac{E'}{E} \frac{l_{\alpha\beta}}{2E} W^{\alpha\beta}, \tag{108}$$

where $l_{\alpha\beta}$ is a lepton spin tensor arising from a sum over all spin states of the leptons

$$l_{\alpha\beta} = l_\alpha l'_\beta + l'_\alpha l_\beta - g_{\alpha\beta}\, l \cdot l' \tag{109}$$

and the hadron structure function is

$$W_{\alpha\beta}(q, p) = \sum_X \int \frac{d^4y}{2\pi} e^{-iq\cdot y} \langle p | J_\alpha(y) | X \rangle \langle X | J_\beta(0) | p \rangle \tag{110}$$

with J_α the electromagnetic current.

Current conservation allows us to write the structure function as

$$W_{\alpha\beta}(q,p) = \left(-g_{\alpha\beta} + \frac{q_\alpha q_\beta}{q^2}\right) W_1(q^2,x) +$$

$$\left(p_\alpha - \frac{(p\cdot q)q_\alpha}{q^2}\right)\left(p_\beta - \frac{(p\cdot q)q_\beta}{q^2}\right) W_2(q^2,x) \tag{111}$$

where $x = -q^2/2p\cdot q$, $\frac{p\cdot q}{m} = \nu = E-E'$ in the laboratory. The two structure functions W_i are related to the cross sections for absorption of transverse or longitudinal virtual photons by

$$\sigma_T(x,q^2) = \left(\frac{4\pi^2\alpha}{m\nu + q^2/2}\right) W_1(q^2,x) \tag{112}$$

and

$$\sigma_L(x,q^2) = \left(\frac{4\pi^2\alpha}{m\nu + q^2/2}\right)\left(-W_1 + m^2\left(1-\frac{\nu^2}{q^2}\right) W_2\right) \tag{113}$$

The kinematics of this process established we may now proceed to model predictions for W_1 and W_2. The picture given by the parton model is that the proton of momentum p moving along the z-axis

$$p = (\sqrt{m^2+p^2}, 0, 0, p) \tag{114}$$

is composed of a bunch of consituents with momentum (see Fig. 17).

$$k_i = (\sqrt{\mu_i^2 + |\underset{\sim}{k}_T|^2 + k_{\ell i}^2}, \underset{\sim}{k}_{Ti}, k_{\ell i}). \tag{115}$$

Each parton is presumed to have finite transverse momentum $\underset{\sim}{k}_T$ and it is convenient to scale its longitudinal momentum

$$k_{\ell i} = \xi_i p. \tag{116}$$

Clearly

$$\sum_i \xi_i = 1 \tag{117}$$

and

$$\sum_i \underset{\sim}{k}_{Ti} = 0. \tag{118}$$

If the frequency of the photon is very large (which in the laboratory means $\nu = E - E'$ is large), then the interaction time for the photon will be short compared to the "binding time" of the partons to make the proton, and we may imagine that the photon interacts individually with the partons. If we further let q^2 become large then the momentum transfered to an individual parton will be so large that in order to make the sum over states in (110) be non-vanishing, the same parton must re-emit the virtual photon. These two requirements: ν large so the individual parton or impulse approximation is suggested and q^2 large so that the inelastic scattering process in coherent (Fig. 18) --these define a physical situation where one may expect to "view" partons.

Under these circumstances we write

$$W_{\alpha\beta}(p,q) = \sum_{N,i} P_N(i)\, w_{\alpha\beta}(k_i, q), \tag{119}$$

where $P_N(i)$ is the probability of finding in the proton N partons of momentum k_i and other quantum numbers, and $w_{\alpha\beta}(k_i, q)$ is the parton structure function. Since we envision the partons to be point-like, the $w_{\alpha\beta}$ are easy enough to evaluate. If the parton of mass μ_i and Q_i has spin zero then

$$w^0_{\alpha\beta}(k_i,q) = Q_i^2 (2k_i+q)_\alpha (2k_i+q)_\beta \delta(\mu_i^2 - (k_i+q)^2), \tag{120}$$

and if it carries spin 1/2

$$w^{1/2}_{\alpha\beta}(k_i,q) = \frac{Q_i^2}{4} tr\left(\gamma_\alpha(\not{k}_i+\not{q}+\mu_i)\gamma_\beta(\not{k}_i+\mu_i)\right)\delta(\mu_i^2-(k_i+q)^2). \tag{121}$$

It is convenient to evaluate these in the frame where q is aligned along the negative z-axis

$$q = (0, 0, 0, \sqrt{-q^2}) \tag{122}$$

In this frame

$$W_{xx} = W_1, \tag{123}$$

and

$$W_{tt} = -W_1 + (m^2 - q^2/4x^2) W_2 . \tag{124}$$

For spin 0 partons we find

$$W^0_{tt} = x \varphi_i^2 \delta(x - \xi_i) + O(1/-q^2), \tag{125}$$

and

$$W^0_{xx} = O(1/-q^2) \tag{126}$$

for large q^2, fixed x. This means

$$W_1^0(x, q^2) \underset{\substack{-q^2 \to \infty \\ x \text{ fixed}}}{\sim} O(1/-q^2) \tag{127}$$

and

$$m\nu W_2^0(x, q^2) \sim 2x^2 \sum_{N,i} P_N(i) \varphi_i^2 \delta(x - \xi_i). \tag{128}$$

This is our first example of <u>scaling</u> which is a general result of the parton model. A structure function which depends on two variables x and q^2 becomes independent of q^2 as $-q^2 \to \infty$ and depends only on the dimensionless variable $x = -q^2/2p \cdot q$. In the spinless parton case the interesting ratio

$$R = \sigma_L/\sigma_T \sim O(-q^2) \tag{129}$$

This last result is in flat contradiction with experimental results which are consistent with R small and possibly zero in the x fixed, $-q^2 \to \infty$ limit.

For spin 1/2 partons we find

$$W_{xx}^{1/2} = \frac{x}{2}\sum_i Q_i^2 \delta(x-\xi_i) + O(1/-q^2), \tag{130}$$

and

$$W_{tt}^{1/2} = O(1/-q^2). \tag{131}$$

This implies

$$W_1^{1/2}(x,q^2) \underset{x \text{ fixed}}{\sim} \frac{x}{2}\sum_{N,i} P_N(i) Q_i^2 \delta(x-\xi_i), \tag{132}$$

and

$$m\nu\, W_2^{1/2} = 2x\, W_1^{1/2} + O(1/-q^2) \tag{133}$$

which leads to

$$R = \sigma_L/\sigma_T = O(1/-q^2) \tag{134}$$

which is in accord with the experimental results.

Let us acquire a little perspective about our calculation which is, in a sense, at the very heart of the parton model and is its principal achievement. We have assumed that high frequency photons with a large q^2 interact with the point like constituents of a hadron as if they are free. This led us directly to the result that dimensionless structure functions (W_1 and νW_2) become dependent on dimensionless quantities (like x) only, as $-q^2 \to \infty$. This makes a great deal of sense because

in a free theory the only scales around are masses and possibly couplings. As momenta become infinite masses, at least, outht to be negligible and the scale of any function ought to be set by appropriate powers of those large momenta. Choosing dimensionless structure functions ought to lead to dependence ondimensionless variables only. This argument is false in an interacting field theory because the renormalization procedure introduces a mass scale which cannot be tossed away and "anomalous" dimensions may result. By assuming the relevance of a free field theory, we have guaranteed a scale invariant set of results.

Now experiments seem to so far bear out the scale invariant behavior of W_1 and νW_2 and the possibility that R is zero or small. This leads one to guess that all partons have spin 1/2- or more precisely all partons interacting with the electromagnetic current have spin 1/2.

The probability density to find a parton with (longitudinal) momentum in a certain piece of x space is directly related to W_2. Phase space is

$$\frac{d^3p}{E} = d^2p_T \frac{dx}{x} \tag{135}$$

for large p, so the probability f(x) that a parton is in x to x + dx is

$$x \sum_{i,N} P_N(i) Q_i^2 \delta(x-\xi_i) = f(x) = \frac{m\nu W_2}{x} , \tag{136}$$

that is

$$\lim_{-q^2\to\infty} m\nu\, W_2(x,q^2) = x f(x). \tag{137}$$

The total number of (charged) partons is

$$\int_0^1 dx\, f(x) = \int_0^1 \frac{dx}{x} F_2(x), \tag{138}$$

where we have called

$$\lim_{\substack{-q^2\to\infty \\ x \text{ fixed}}} m\nu\, W_2(x,q^2) = F_2(x) \tag{139}$$

and noted that physical phase space involves $0 \le x \le 1$. The experimental shape of $F_2(x)$ is indicated in Fig. 20. Near $X = 1$, very fast partons, $f(x) \approx (1-x)^3$ while for slow partons $f(x)$ seems to behave as $1/x$ which, if correct, would mean that in a proton at infinite momentum there are a logarithmically infinite number of partons.

One can now apply the basic parton idea to many processes. We shall pass this up and refer the reader to the references and instead discuss some of the consequences of the very attractive idea that the spin 1/2 partons are nomeother than the quarks of Gell-Mann and Zweig. One is immediately faced with the logical probelm that if partons (quarks) are constituents of hadrons, how it it that they do not escape from hadrons on being struck so violently in inelastic lepton scattering? Since no one has ever seen a quark, they had better stay in. Well, no one knows! But we'll simply shove this problem under the rug and ignore it.

If the various consequences of assuming partons are quarks are true, one must reopen the issue.

So we imagine that there are densities u(x), d(x), and s(x) for finding up (Q = 2/3, S = 0), down (Q = -1/3, S = 0) and strange (Q = 1/3, S = -1) quarks in the proton and similarly anti-quarks. The charge on a proton being one means

$$1 = \int_0^1 dx \left\{ \frac{2}{3}(u(x)-\bar{u}(x)) - \frac{1}{3}(d(x)-\bar{d}(x)) - \frac{1}{3}(s(x)-\bar{s}(x)) \right\} , \tag{140}$$

while conservation of isospin means

$$\frac{1}{2} = \int_0^1 dx \left\{ \frac{1}{2}(u(x)-\bar{u}(x)) - \frac{1}{2}(d(x)-\bar{d}(x)) \right\} , \tag{141}$$

and the absence of strangeness means

$$\int_0^1 dx \left\{ s(x) - \bar{s}(x) \right\} = 0 \tag{142}$$

The structure function for electron scattering on protons is

$$\frac{m\nu W_2^{ep}(x)}{x} = F_2^{ep}(x) =$$

$$\frac{4}{9}(u(x)+\bar{u}(x)) + \frac{1}{9}(d(x)+\bar{d}(x)) + \frac{1}{9}(s(x)+\bar{s}(x)) , \tag{143}$$

and on neutrons

$$f^{en}(x) = \frac{1}{9}\left\{4u(x) + \bar{u}(x)\right\} + \frac{4}{9}\left\{d(x) + \bar{d}(x)\right\} + \frac{1}{9}\left\{s(x) + \bar{s}(x)\right\}, \tag{144}$$

since ups and downs change from proton to neutron. This gives us a first result, namely

$$4 \geq F_2^{ep}(x) \Big/ F_2^{en}(x) \geq \frac{1}{4} \tag{145}$$

if the quark parton model is correct. The experimental evidence is consistent with these bounds, and the ratio seems to be very close to 1/4 near x = 1. Unfortunately thatis just the region where separation of the neutron structure functions from deuterium has the largest ambiguity. But the model seems OK.

Another consequence for our choice of partons comes from momentum conservation which says that if charged quarks carry all the momentum of the proton, then

$$1 = \int_0^1 dx\ x\left\{u(x) + \bar{u}(x) + d(x) + \bar{d}(x) + s(x) + \bar{s}(x)\right\} \tag{146}$$

From the experimental shape of $f^{ep}(x)$ and $f^{en}(x)$, one has

$$\int_0^1 dx\ x\, f^{ep}(x) = 0.18, \tag{147}$$

and

$$\int_0^1 x\, f^{en}(x)\, dx = 0.13 \tag{148}$$

Combining these one finds

$$\int_0^1 dx\ x\left\{q(x) + \bar{q}(x)\right\} = 0.72 \tag{149}$$

which would mean that over 70% of the proton momentum is carried by strange charged quarks. The conclusion obviously is that there is present in the proton a large amount of uncharged partonic matter and that most of the proton's momentum is stashed there.

Now we will end the discussion of partons by saying a few words about neutrino induced inelastic reactions and derive some sum rules which test the quark parton idea.

Inelastic neutrino scattering on a nucleon is the inclusive process $\nu_\ell + N \to \ell$ + anything. The structure functions involved here are three in number and are given by the tensor structure

$$W_{\alpha\beta}(p,q) = -g_{\alpha\beta} W_1(q^2,x) + p_\alpha p_\beta W_2(q^2,x) - i\,\varepsilon_{\alpha\beta\sigma\tau} q^\sigma p^\tau W_3(q^2,x). \tag{150}$$

The new function enters because of vector-axial vector interference terms in the weak cross section. The differential cross section for incident neutrinos is given in terms of the W_i by

$$\frac{d\sigma(\nu+p\to l+\text{anything})}{dx\,dy} = \frac{G_F^2 m}{\pi} E\left\{xy^2 \tilde{F}_1(x,q^2) + \left(1-y-\frac{mxy}{2E}\right)\tilde{F}_2(x,q^2) - xy\left(1-y/2\right)\tilde{F}_3(x,q^2)\right\}, \tag{151}$$

where $y = \nu/E$, E is the incident neutrino energy, G_F is the Fermi coupling constant, and

$$\tilde{F}_1(x,q^2) = W_1(x,q^2), \tag{152}$$

$$\tilde{F}_2(x,q^2) = m\nu\, W_2(x,q^2), \tag{153}$$

and

$$\tilde{F}_3(x,q^2) = m\nu\, W_3(x,q^2). \tag{154}$$

These functions $\tilde{F}_i(x,q^2)$ are the combinations of ν and the W_i which both naive dimensional arguments and the kindergarten parton model we have outlined would suggest satisfy the Bjorken scaling hypothesis

$$\lim_{\substack{-q^2\to\infty \\ x \text{ fixed}}} \tilde{F}_i(x,q^2) = F_i(x), \tag{155}$$

where the $F_i(x)$ are non-vanishing functions of x. If this scaling occurs, then integrating over x and y in (151) to get the total neutrino proton cross section one finds

$$\sigma_\nu(E) = A\,E, \tag{156}$$

that is, the cross section rises linearly with the incident neutrino energy. The latest data from CERN indicates that this linear rise is in fact consistent though not compelling. They find for 2 GeV ≤ E ≤ 10 GeV

$$\sigma_\nu(E) = 0.74\,(E \text{ in GeV}) \times 10^{-38}\ \text{cm}^2 \tag{157}$$

and for anti-neutrinos (change the sign of F_3) the data are consistent with

$$\sigma_{\bar\nu}(E) = 0.28\,(E \text{ in GeV}) \times 10^{-38}\ \text{cm}^2. \tag{158}$$

So the indications are, so far, that scaling works even at the remarkably low q^2 values available in present experiments.

Now we'll proceed again as if the partons were quarks and derive some sum rules to be checked by further neutrino data from CERN and NAL. Using our assignments of quantum numbers for the quarks the weak current is written

$$j_\alpha = \cos\vartheta_c\ \bar\psi_u \gamma_\alpha (1-\gamma_5)\psi_d + \sin\vartheta_c\ \bar\psi_d \gamma_\alpha (1-\gamma_5)\psi_s, \tag{159}$$

with ϑ_c the Cabbibo angle presumed to be the same for quark-partons as other hadrons. Using this current leads to

$$f_1^{\nu p}(x) = \bar u(x) + d(x)\cos^2\vartheta_c + s(x)\sin^2\vartheta_c, \tag{160}$$

$$f_1^{\bar\nu p}(x) = u(x) + \bar d(x)\cos^2\vartheta_c + \bar s(x)\sin^2\vartheta_c, \tag{161}$$

$$f_2^{\nu n}(x) = \bar d(x) + u(x)\cos^2\vartheta_c + s(x)\sin^2\vartheta_c, \tag{162}$$

$$f_1^{\bar{\nu}n}(x) = d(x) + \bar{u}(x)\cos^2\vartheta_c + \bar{s}(x)\sin^2\vartheta_c \tag{163}$$

and many more.

From these follow

$$\int_0^1 dx \left(f_1^{\bar{\nu}p} - f_1^{\nu p}\right) = 2 - \cos^2\vartheta_c \approx 1 \tag{164}$$

which is the old Adler neutrino sum rule which is not testing the quark model. A sum rule which does test the quark model is

$$\int_0^1 dx \left[f_3^{\nu n} + f_3^{\bar{\nu}n}\right] = -2\left(1 + 2\cos^2\vartheta_c\right) \approx -6 \tag{165}$$

and there are others. Experimental data to check these sum rules is not yet extant.

The parton model is presented here is a very simple idea with really a small number of consequences. One can apply the model to a host of other processes involving currents such as $e^+e^- \rightarrow$ hadrons or $pp \rightarrow \mu^+\mu^-$ + anything, but the tests of the results of such applications are still being carried out. With additional assumptions, particularly on the manner in which quark-partons somehow transmute themselves into hadrons without transmitting their curious and unobserved quantum numbers to the external world, one may derive parton model results which relate to strong interaction processes alone. A realm of particular interest of late has been inclusive processes at large transverse momentum. It is possible that the guts of this reaction involves

some kind of basic parton-parton interaction which is only gently sh shielded as the partons transmute to hadrons. This topic and others involving detailed applications to current-hadron interactions I leave to the reader of the references.

REFERENCES

Multiperipheral Model -- Selected useful references

[1]D. Amati, A. Stanghellini, and S. Fubini, Nuovo Cimento 26, (896) 1962. A basic and valuable source.

[2]G. F. Chew, Lectures at the Brookhaven National Laboratory Summer School, 1970. A good introduction into modern ideas on multiperipheralism.

[3]H. D. I. Abarbanel, G. F. Chew, M. L. Goldberger, and L. M. Saunders, Ann. Phys. (N. Y.) 73, 156 (1972). More modern developments in the multiperipheral model with attention focused on inclusive reactions.

[4]C. de Tar, Phys. Rev. D3, 128 (1971). A very good exposition of inclusive processes in many models.

[5]For experimental data relevant to the multiperipheral model, consult the recent review by M. Jacob, CERN preprint, TH-1683, July 1973.

Parton Model

[1]R. P. Feynman, Photon-Hadron Interactions (W. A. Benjamin, Inc., 1972). Partons and many related topics.

[2]J. D. Bjorken, Phys. Rev. 179, 1547 (1969). Scaling

FIGURE CAPTIONS

Fig. 1 Elastic scattering kinematics.

Fig. 2 Peripheral amplitude for 2→2 processes.

Fig. 3 2→3 amplitude kinematics.

Fig. 4 Kinematics for peripheral amplitude for 2→3 reaction

Fig. 5 Multiperipheral kinematics for the 2→n amplitude.

Fig. 6 The n particle contribution to the s-channel unitarity relation.

Fig. 7 Multiperipheral contribution to the n-particle s-channel unitarity relation.

Fig. 8 Multiperipheral recursion relation.

Fig. 9 Kinematics for the multiperipheral integral equation.

Fig. 10 Single particle inclusive process.

Fig. 11 The A fragmentation region in the multiperipheral model.

Fig. 12 The multiperipheral contribution to the central region of rapidity space.

Fig. 13 Reggeons replacing the multiperipheral absorptive parts in Fig. 12.

Fig. 14 Prediction of the multiperipheral model for the

distribution in rapidity for a single particle inclusive reaction. Shown in the center of mass frame.

Fig. 15 Triple-Regge diagram for the single particle inclusive reaction at the edge of physical phase space.

Fig. 16. Kinematics of deep inelastic electron scattering.

Fig. 17 A proton of momentum p and its partons of momentum k_i.

Fig. 18 Electroproduction in the parton model showing the coherent interaction of the virtual photon with an individual parton.

Fig. 19 The photon-parton structure function $W_{\alpha\beta}(k_i q)$.

Fig. 20 The structure function νW_2 in the scaling limit. This is a casual representation of the experimental data.

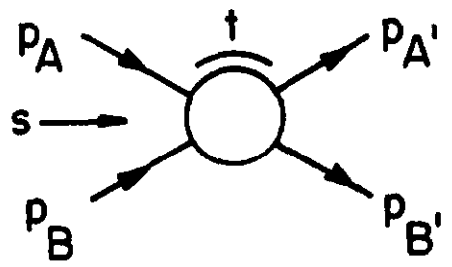

$$s = (p_A + p_B)^2$$

$$t = (p_A - p_{A'})^2$$

Fig. 1

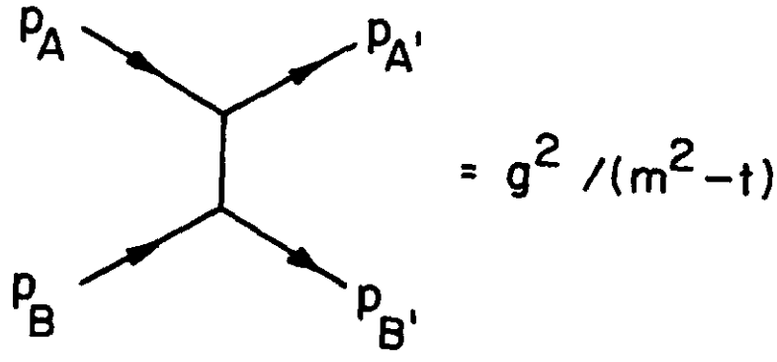

Fig. 2

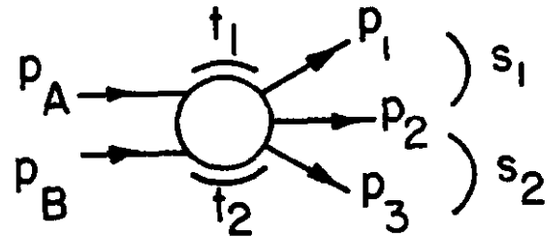

Fig.3

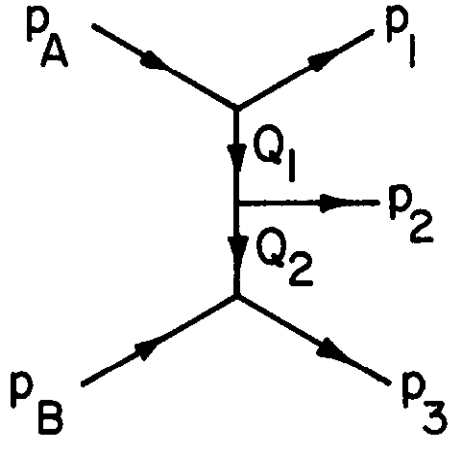

Fig.4

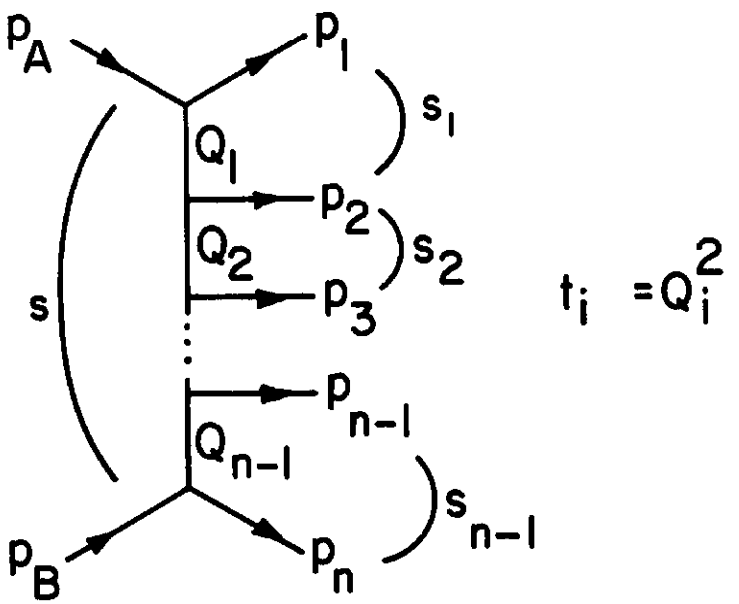

Fig. 5

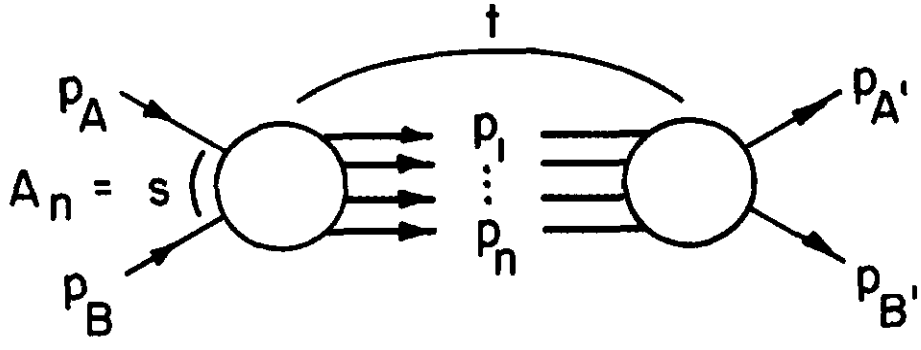

Fig. 6

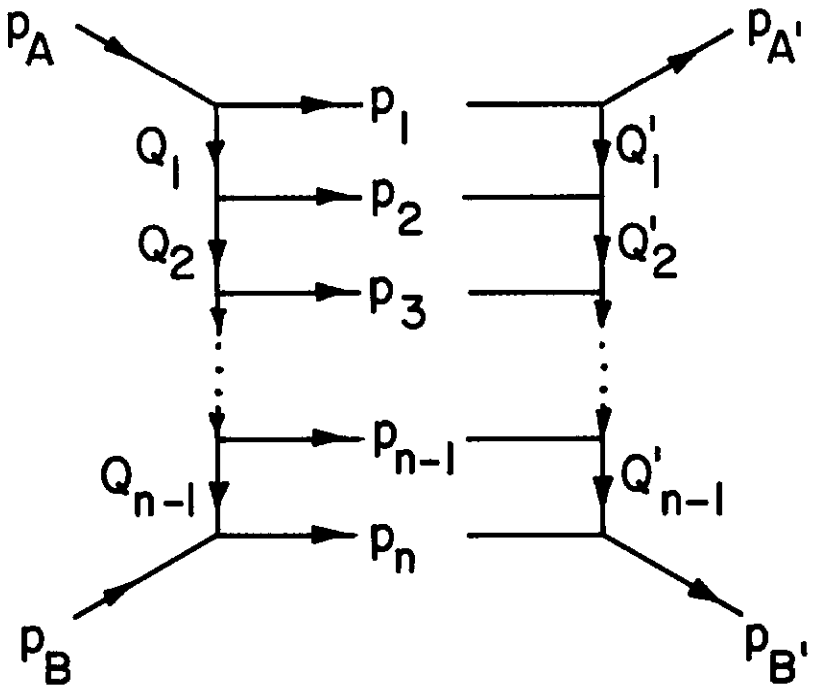

Fig. 7

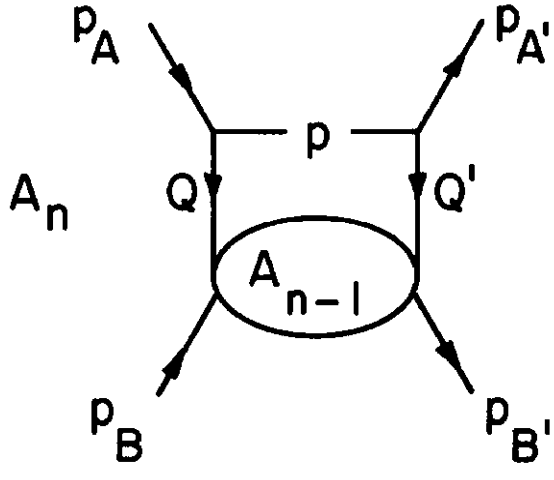

Fig.8

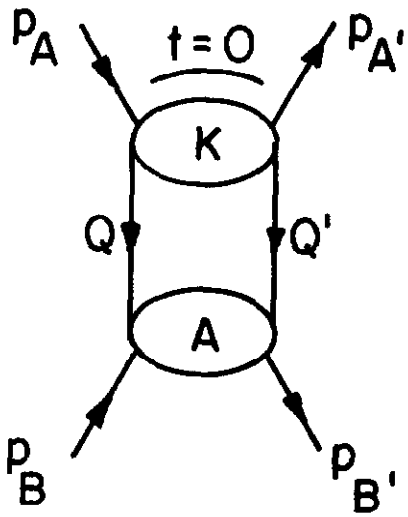

Fig. 9

$$p_A^2 = U \qquad s = (p_A + p_B)^2$$

$$Q^2 = U \qquad s_0 = (p - Q)^2$$

$$p_B^2 = V \qquad s' = (Q + p_B)^2$$

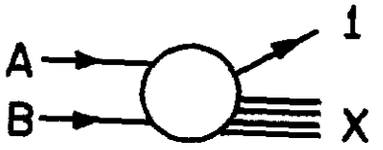

Fig. 10

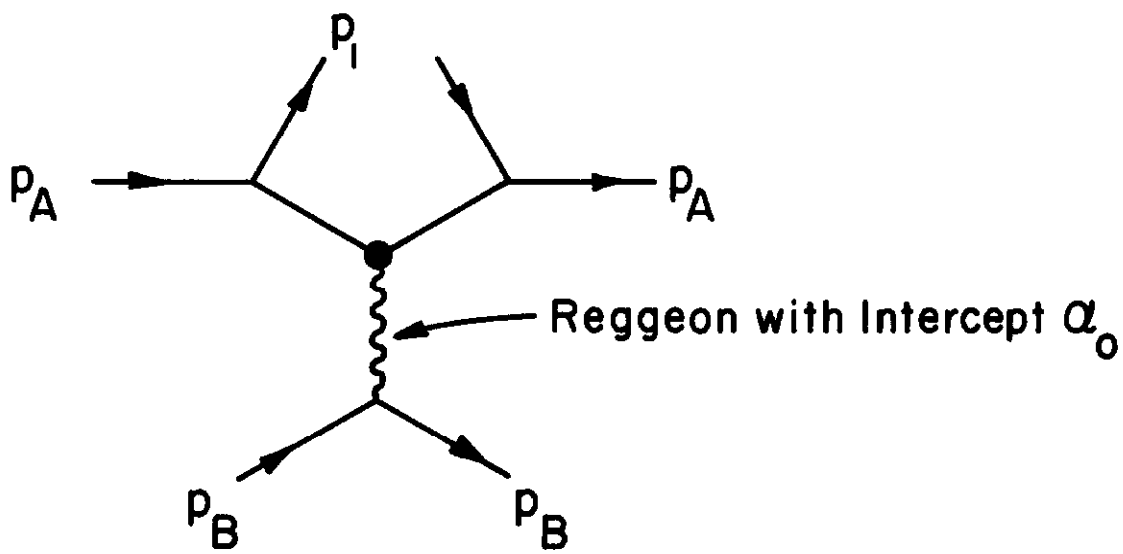

Fig. 11

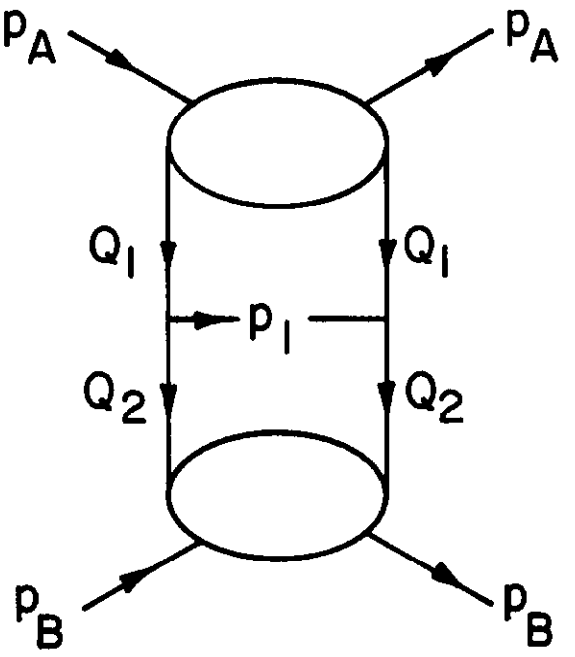

Fig. 12

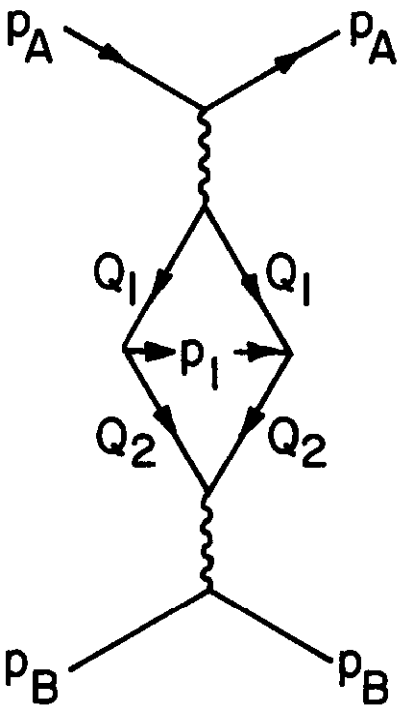

Fig. 13

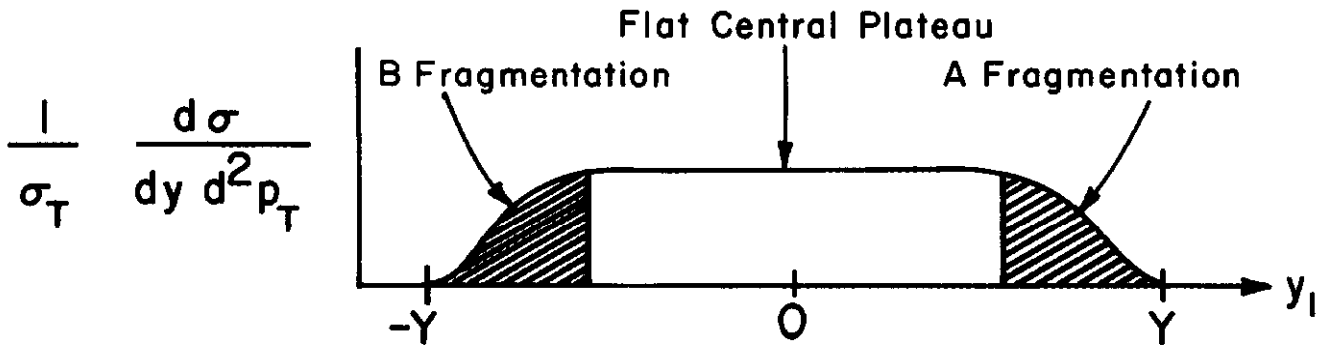
$\frac{1}{\sigma_T} \frac{d\sigma}{dy\, d^2p_T}$
Flat Central Plateau
B Fragmentation
A Fragmentation
-Y
0
Y
y_1

Fig. 14

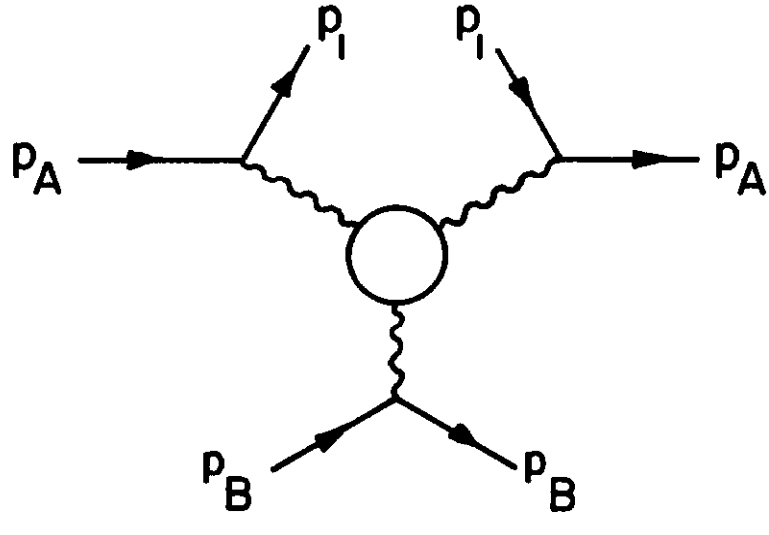

Fig. 15

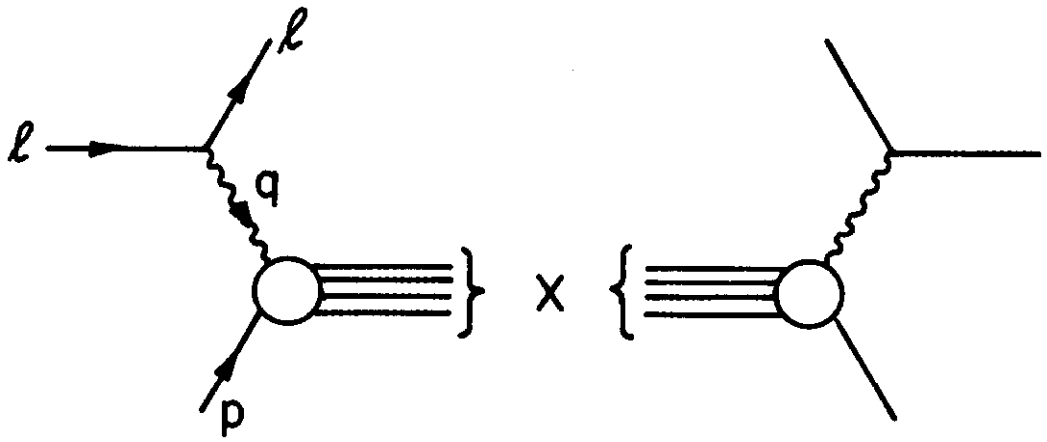

Fig. 16

Fig. 17

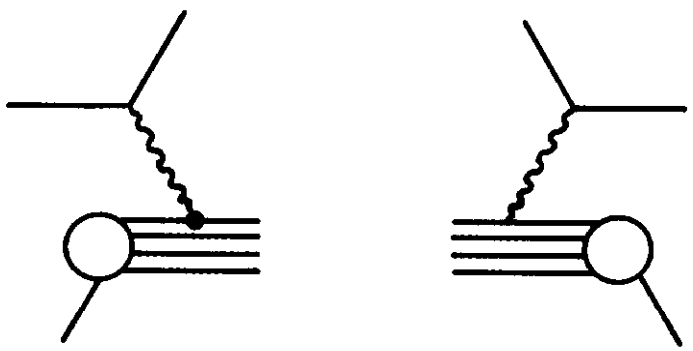

Fig. 18

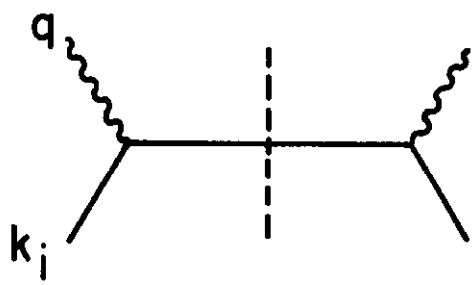

Fig. 19

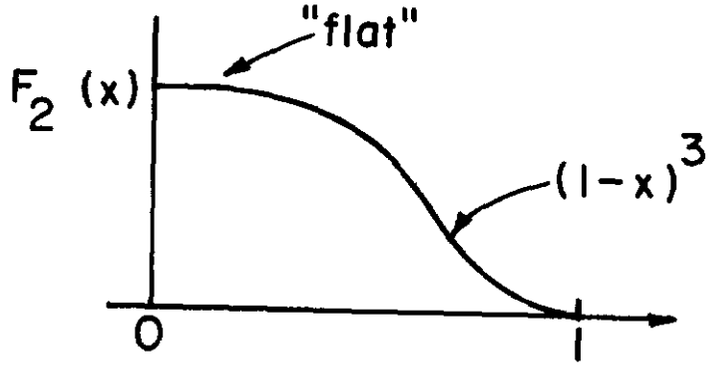

Fig. 20